Thermal and Mechanical Characterization of EVA/Banana Fiber-Derived Cellulose Composites

E. K. Silviya,[1] G. Unnikrishnan,[1] S. Varghese,[2] J. T. Guthrie[3]

[1]*Department of Chemistry, National Institute of Technology, Calicut 673601, India*
[2]*School of Nanoscience and Technology, National Institute of Technology, Calicut 673601, India*
[3]*Department of Colour Science, School of Chemistry, University of Leeds, LS2 9JT, United Kingdom*

Received 27 September 2010; accepted 25 June 2011
DOI 10.1002/app.35140
Published online 28 December 2011 in Wiley Online Library (wileyonlinelibrary.com).

ABSTRACT: Composite films based on poly(ethylene-*co*-vinyl acetate) (EVA) and cellulose derived from banana plant waste have been prepared and characterized. Cellulose whiskers isolated from, banana fibers, by an acid hydrolysis method and were incorporated into the EVA matrix by solution casting technique. The composite films were subsequently examined by scanning electron microscopy, thermogravimetry, differential scanning calorimetry, and FTIR spectroscopy. Compared with pure EVA and cellulose, the EVA/cellulose composite systems showed superior thermal stability. The mechanical testing of the composite films revealed that the tensile strength and elastic modulus were increased after cellulose incorporation into EVA. Among the EVA/cellulose composites, 7.5% cellulose loaded EVA showed the highest tensile strength. The percentage strain at break of the EVA/cellulose composite systems was found to be decreased which has been attributed to the restricted mobility of the polymer matrix by the presence of cellulose. X-ray diffraction studies showed that the EVA/cellulose composites were more crystalline than EVA. © 2011 Wiley Periodicals, Inc. J Appl Polym Sci 125: 786–792, 2012

Key words: polymer nanocomposites; fibers; thermal properties; mechanical properties; casting

INTRODUCTION

The use of cellulosic fibers for the fabrication of novel composites has attracted much interest because of their ecological and renewable features. When compared with mineral fillers, cellulose fibers offer a number of benefits which include high-specific stiffness and improved strength, flexibility during processing with no harm to the equipment, low density, biodegradability, and low cost. Several cellulosic products and wastes such as sugar cane baggase, flax yarns, sisal fiber, and wood powder have been used as fillers in thermoplastics.[1–3]

Favier et al. were the first to demonstrate the benefits of reinforcing a polymer with cellulose whiskers.[4] Cellulose whiskers, derived from tunicate cellulose, were incorporated into a styrene–butyl acrylate latex. The resulting composite films showed a twofold increase in shear modulus over the control films that contained no whiskers. Following this observation, several other synthetic polymers and natural polymers, including poly(vinylchloride),[5–7] polypropylene,[8] polyoxyethylene,[9–11] starch,[12] poly(lactic acid)[13] and cellulose acetate butyrate have been beneficially reinforced with cellulose whiskers. The results of these type of studies and those of others have been summarized in an impressive review by Samir et al.[14]

Cellulose nanofibrils, from different sources and in different forms, have been used to develop nanocomposites in combination with several different polymer matrices. To obtain a significant increase in material properties, the cellulose whiskers need to be well separated and evenly distributed in the matrix material. The polar nature of cellulose often prevents its uniform distribution in nonpolar media during the casting process, a usually followed route to develop composite systems. However, a few published methods describing the re-dispersion of cellulose microfibres/nanofibres in polar and nonpolar organic liquids are available. For example, Heux et al. developed a facile and reproducible method for obtaining stable suspensions of cellulose in nonpolar organic liquids (toluene and cyclohexane) using BNA (a phosphoric ester surfactant) as a stabilizing agent.[15] Gousse et al. redispersed cellulose nanocrystals in nonpolar organic liquids by partially silylating their surface.[16] Grunert and Winter used the same strategy to redisperse cellulose nanocrystals in acetone.[17] A study by Araki et al. showed that grafting low molecular weight poly(ethylene glycol) onto the surface of cellulose whiskers could lead to a stable suspension in chloroform.[18] Samir et al. redispersed tunicin whiskers in a polar organic

Correspondence to: G. Unnikrishnan (unnig@nitc.ac.in).
Contract grant sponsor: UK-India Education Research Initiative program (UKIERI).

© 2011 Wiley Periodicals, Inc.

fluid, dimethyl formamide (DMF), without the need for surfactants or any chemical modifications, for use in polymer reinforcement.[19] The authors proposed that the stability of suspension was due to the high dielectric constant of DMF and the medium wettability of tunicin whiskers. Later, Viet et al. examined the dispersion of cellulose nanocrystals in the polar organic solvents, DMF and DMSO.[20] The authors found that the re-dispersion was incomplete. There was some evidence for the aggregation in the suspensions. The presence of a small amount of water appeared to be critical to the suspension stability.

Banana fiber, a fibrous residue of pseudostems and leaves left over after banana cultivation is one of the rich sources of cellulose. Banana cultivation generates a considerable amount of agricultural waste, causing environmental problems in banana farming regions. This residual resource of cellulose has attracted much interest due to the potential use of such materials as a reinforcing component in high performance composite materials. The isolation of cellulose from banana fibers involves the removal of hemicellulose, lignin, pectin, etc., that are present along with cellulose. This can be achieved by an alkaline pretreatment and bleaching. Cellulose whiskers can be obtained by a further acid hydrolysis treatment.

Among the numerous ethylene copolymers, poly(ethylene-*co*-vinyl acetate) (EVA), finds wide range of applications, ranging from adhesives to cable insulators.[21] EVA is available with vinyl acetate levels typically in the range 3–50% w/w. The commercial success of EVA is due to its transparency and its ease of fabrication. Moreover, it is heat processable, flexible, and relatively inexpensive. The safety and biocompatibility of EVA copolymers are indicated by its use as a biomaterial for artificial hearts and as an antithrombogenic material.[22]

The objectives of this work are to isolate cellulose whiskers from banana plant fibers and to utilize the whiskers to modify the features of EVA. The isolated cellulose whiskers were dispersed in tetrahydrofuran (THF) by frequent sonication and magnetic stirring. Composite films were prepared by casting a mixture of the cellulose dispersion in THF and the EVA-THF solution. The composite films have been characterized by FT-IR spectroscopy, differential scanning calorimetry (DSC), thermogravimetry (TGA), X-ray diffraction (XRD), and in terms of their mechanical properties.

EXPERIMENTAL

Materials

Banana fibers were supplied by the Fiber Design Centre, Khadi and Village Industries Commission (KVIC), Trivandrum, India. They were used as the source of cellulose whiskers. Sulfuric acid (>98%) was obtained from Fisher Scientific, UK. Poly(ethylene-*co*-vinyl acetate) (EVA-1802) (vinyl acetate content = 18%) was supplied by National Organic and Chemical Industries Limited (NOCIL) Mumbai, India. The chemicals used for the pretreatment of banana fibers were of analytical purity. Tetrahydrofuran (THF) was purchased from Sigma Aldrich, Switzerland. The solvents used for the contact angle measurement were of analytical grade, supplied by Fisher Scientific (UK).

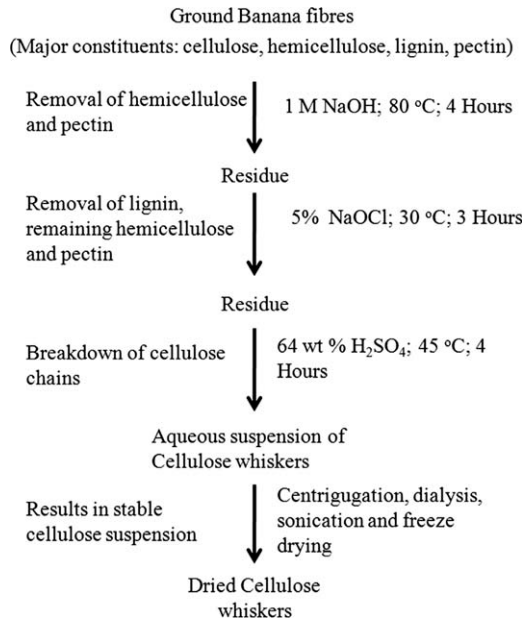

Figure 1 Schematic representation for the isolation of cellulose from banana fibers.

Development of poly(ethylene-*co*-vinyl acetate)/cellulose composite films

Isolation of cellulose whiskers from banana fibers

Cellulose derived from banana waste fibers were used as the filler in EVA matrix. The cellulose whiskers were generated from the banana fibers by an acid catalyzed hydrolysis. A schematic representation of the isolation process is shown in Figure 1. The ground banana fibers were subjected to alkali treatment and bleaching prior to acid hydrolysis. The pretreated banana fibers were then treated with 64 wt % sulfuric acid solution at 45°C for 4 h. After hydrolysis, the mixture was diluted 10-fold with deionized water and neutralized with an alkaline solution, and then subjected to centrifugation. The suspension was dialyzed with deionized water and sonicated for 30 min in an ultrasonic bath. This suspension was freeze dried in a freeze drier (LSL Secfroid, Switzerland). A detailed procedure for the isolation of cellulose from banana fibers by using

TABLE I
Formulation of EVA/Cellulose Composites

Sample	Amount of cellulose (g)	Amount of EVA (g)	% weight of cellulose
EVA	0	3	0
EVA/Cell. 2.5%	0.0770	3	2.5
EVA/Cell. 5.0%	0.1580	3	5.0
EVA/Cell. 7.5%	0.2433	3	7.5
EVA/Cell. 10%	0.3340	3	10.0

different reaction conditions have been discussed in a previous article by the authors.[23]

Preparation of EVA/cellulose composites

Three grams EVA was dissolved in 50 g of THF by heating at 60°C for 4 h under vigorous stirring. The excessive solvent vaporization was prevented by using a reflux condenser. In a parallel exercise, a dispersion of the cellulose whiskers was prepared by separately weighing a known amount of the previously freeze dried cellulose sample. Dispersions with different wt % (varying from 0 to 10%) of cellulose in THF were mixed with EVA-THF solution. This mixture was further heated for 10 min at 60°C, while being stirred mechanically. The dispersion was casted in glass molds (17 cm × 17 cm × 0.5 cm) and dried at room temperature in a fume cupboard. The films were of 50 ± 10 μm in thickness. The formulation used in the composite preparation is given in Table I.

Characterization

Cellulose whiskers and solution-casted films were examined by FTIR spectroscopy over the wave number range of 400–4000 cm^{-1} using a Perkin–Elmer Spectrum One spectrometer. X-ray diffraction studies of cellulose whiskers and solution casted films were performed on a PANalytical X'Pert PROMPD system in a 2θ range between 5° and 70°. The morphology of cellulose whiskers and the composite films were investigated by Scanning Electron Microscopy (SEM). The samples were sputter coated with gold to avoid subsequent charging before measurement by SEM. Images were taken at an accelerating voltage of 5 kV, using a JEOL JSM-820 model SEM. EVA/cellulose composite films were analyzed by TGA and DSC. A TGA 2050 series Thermogravimetric analyzer (TA Instruments) across a temperature range 30–500°C, at a heating rate of 10°C/min, in a nitrogen environment, was used for the analysis. The melting temperature of each sample was recorded using a Differential Scanning Calorimetry (DSC 2010 series, TA Instruments) from −50 to 150°C with a heating rate of 10°C/min. The mechanical properties of the composite films were studied by using a Universal Testing Machine (Instron corp., Canton, MA), following the ASTM D 882-88 protocol. The initial grip separation and crosshead speed were set at 40 mm and 50 mm/min, respectively. Tensile strength, percentage strain at break, and elastic modulus were obtained from tensile testing. The data reported are the average of at least five experiments. The critical surface tension of each of the films was determined using the contact angle evaluation approach. Measurements were taken on a Contact-θ-Meter (Pearson Panke, UK) using a range of solvents (1-decanol, nitromethane, formamide and glycerol) at 20°C. The reported contact angles are the average of five measurements. The transmittance of the films was measured by using a MINOLTA Spectrophotometer (Model CM 3600 d), over the range 400–700 cm^{-1}.

RESULTS AND DISCUSSION

FTIR spectroscopy analysis

Figure 2 shows the FTIR spectra of untreated banana fibers, cellulose whiskers, EVA/cellulose 10% composite and pure EVA. The lack of bands at 1731, 1513, and 1239 cm^{-1} in the spectrum of cellulose whiskers indicates the removal of most of the hemicellulose and lignin from the untreated fibers. The —C—O—C— pyranose ring skeletal vibration gives a prominent band at 1022 cm^{-1} in both (a) and (b). The enhanced intensity of this band in spectrum (b) shows the increase in cellulose content in the isolated cellulose whiskers. The band at 896 cm^{-1} in

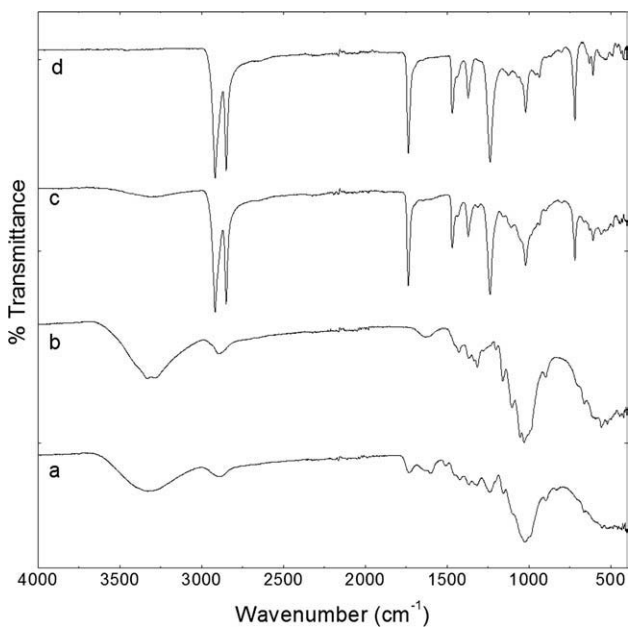

Figure 2 FT-IR spectra of (a) Banana fibers, (b) Cellulose whiskers, (c) EVA/cellulose 10% composite, (d) EVA.

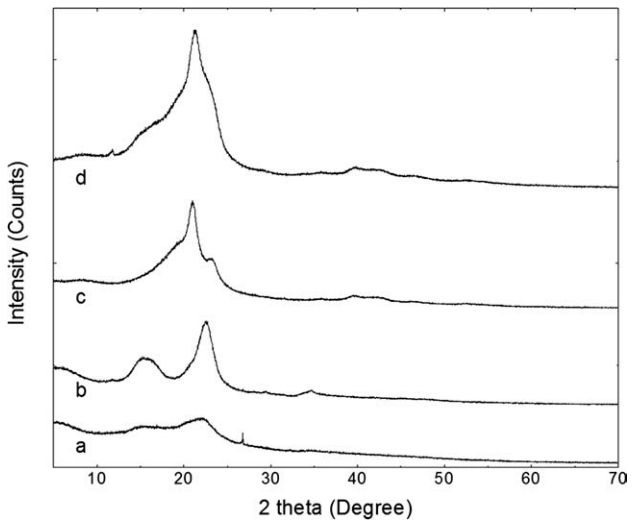

Figure 3 XRD curves of (a) Banana fibers, (b) Cellulose whiskers, (c) EVA, (d) EVA/cellulose 10% composite.

the spectrum of the cellulose whiskers belongs to the typical structure of cellulose.[24]

The peaks at 2927 and 2845 cm^{-1}, in the spectra of EVA samples, have been attributed to the asymmetric and symmetric vibrations respectively, of aliphatic groups $(—CH_2—)_n$. The 1734 cm^{-1} peak corresponds to carbonyl stretching vibrations of acetate groups in EVA. In the case of EVA/cellulose composite, a slight decrease in the intensity of this peak has been observed. It is evident that the addition of cellulose into EVA matrix enhances the width and intensity of the peak at 3600–3000 cm^{-1} (—O—H vibration in cellulose) and 1022 cm^{-1} (—C—O—C— pyranose ring skeletal vibration in cellulose).

X-ray diffraction studies

Figure 3 shows the XRD curves of untreated banana fibers, cellulose whiskers, EVA and 10 wt % cellulose

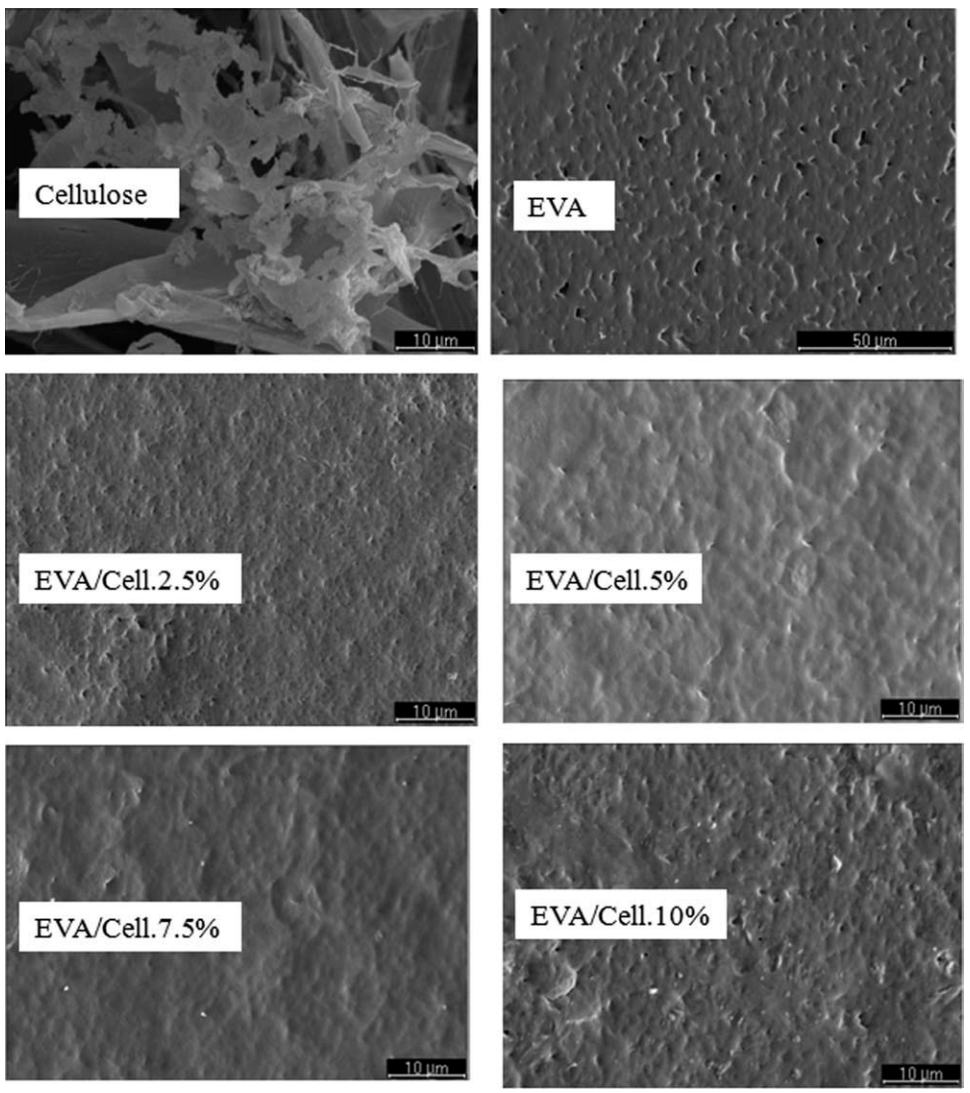

Figure 4 SEM images of freeze dried cellulose, EVA, and EVA/cellulose composites.

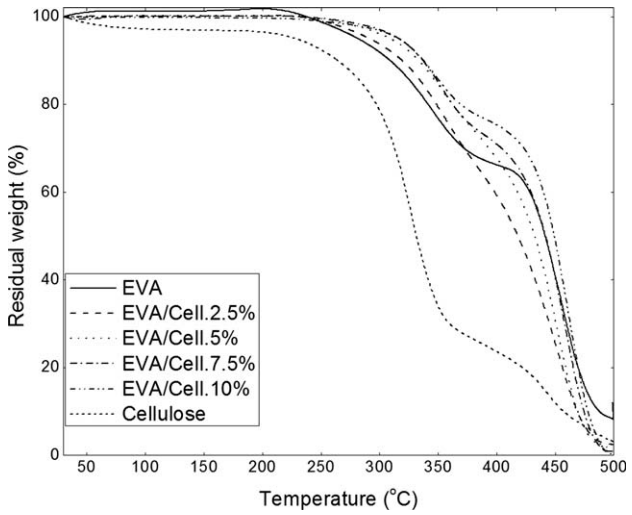

Figure 5 TGA plots of cellulose, EVA, and EVA/cellulose composites.

loaded EVA composite. Comparing the XRD curves of untreated banana fibers and of cellulose whiskers, it is clear that the cellulose obtained after hydrolysis is more crystalline than the untreated banana fibers. The increase in the overall crystallinity of the hydrolyzed fibers has been attributed to the removal of the hemicellulose and lignin during the chemical treatment. For EVA film, a peak has been observed at 21°. In the case of EVA/cellulose composite, the intensity of this peak is found to be increased. This observation shows the enhanced crystallinity of the composites with cellulose incorporation.

Scanning electron microscopy

Figures 4 show the SEM images of cellulose whiskers, EVA and EVA-cellulose composite films. The SEM image of the freeze dried cellulose represents the particles as flakes. However, the particle size analysis of the aqueous suspension of the same sample reveal that the particles are in nanodimension. Further, the freeze drying of the cellulose dispersion could have resulted in the aggregation of cellulose particles. From the SEM images of EVA and cellulose loaded EVA systems, it is clear that up to 7.5 wt % of cellulose loading, homogenous distribution of cellulose in the matrix was possible. At 10 wt % of cellulose loading, cellulose particle-cellulose particle interaction increases and filler starts to agglomerate in the matrix.

Thermal analysis

Figure 5 shows the TGA curves of cellulose, EVA and EVA/cellulose composites. EVA/cellulose composites and the pure components show a two-step degradation profile. In the case of cellulose, there is a weight loss of about 3%, during heating to 120°C. This corresponds to the vaporization and removal of bound water in the cellulose samples. The cleavage of glycosidic linkages of cellulose occurs in the temperature range of 230–370°C. After 380°C, the residual decomposition products maintain a slow degradation profile. The TGA curve of EVA shows two different degradation pathways. The first degradation corresponds to the decomposition of vinyl acetate, which starts at about 280°C. The second degradation occurs over the temperature range of 410–500°C, which corresponds to the scission of the main chain, poly(ethylene) backbone.

The degradation of EVA/cellulose composites starts at a higher temperature than the pure cellulose and EVA. That is, EVA/cellulose composites are more thermally stable than either cellulose or EVA. The onset temperature of degradation and temperature at which maximum degradation occur (DTG peak temperature) that are obtained from the derivative weight loss curve versus temperature plots are presented in Table II. From the Table it can be seen that the onset temperature of degradation of EVA/cellulose composites has been shifted to a higher temperature as the cellulose content varies between 2.5–10 wt %. This can be attributed to the polar–polar interaction between cellulose and vinyl acetate part of EVA. However, the DTG peak temperature has been found to be independent of the cellulose content in the matrix. The second degradation temperature of the EVA/cellulose composites is found to increase with an increase in the cellulose content

TABLE II
DTG Data of EVA, Cellulose, and EVA/Cellulose Composites

	First degradation		Second degradation	
Samples	Onset temperature of degradation (°C)	DTG peak temperature (°C)	Onset temperature of degradation (°C)	DTG peak temperature (°C)
Cellulose	230	326	410	443
EVA	280	345	410	466
EVA/Cell.2.5%	285	355	392	450
EVA/Cell.5%	301	355	397	451
EVA/Cell.7.5%	307	353	403	458
EVA/Cell.10%	309	352	404	461

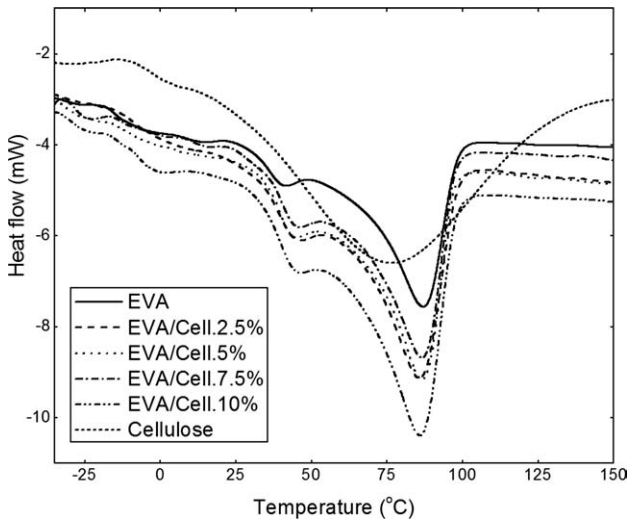

Figure 6 DSC plots of cellulose, EVA, and EVA/cellulose composites.

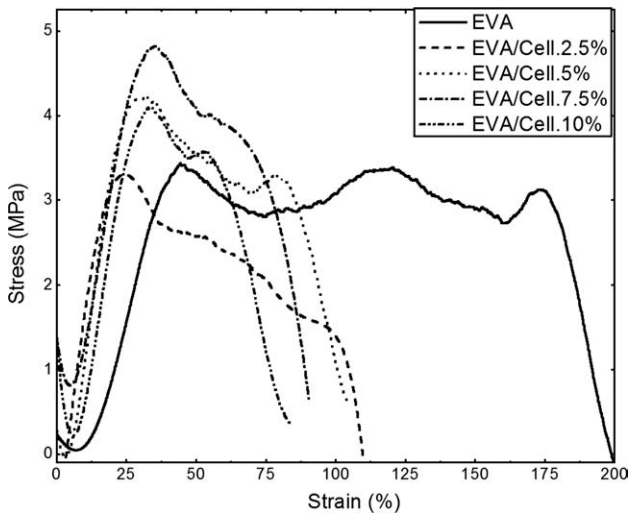

Figure 7 Stress versus strain plots of EVA/cellulose composites.

in EVA matrix, which is expected due to the char formed, during first degradation of cellulose may inhibit the subsequent degradation of the composites.

Figure 6 shows the DSC curves of EVA/cellulose composites. The curves highlight two endothermic peaks; a minor peak corresponding to the softening of vinyl acetate blocks (T_{m1}) and a major peak corresponding to the melting of ethylene blocks (T_{m2}) of EVA, respectively. The values of T_{m1}, T_{m2}, and T_g (glass transition temperature) are presented in Table III.

The melting temperature T_{m1} of EVA/cellulose composites has been found to be shifted to a higher temperature compared to pure EVA. The value of T_{m1} has been observed to be higher by 5°C in the composites and is independent of the cellulose loading in the matrix. This may be due to the nucleation effect of cellulose during the crystallization of EVA matrix. XRD results further support this observation. However, Tm_2 of EVA/cellulose composites has been found to be not affected by the cellulose content in EVA. From this it can be inferred that the added cellulose could be interacting with the vinyl acetate part of EVA and not with the ethylene part. The increase in glass transition temperature of the composites also supports the possible interaction between the hydroxyl groups of cellulose and the vinyl acetate part of EVA.

TABLE III
DSC Data of EVA and EVA/Cellulose Composites

Samples	T_{m1} (°C)	T_{m2} (°C)	T_g (°C)
EVA	41.39	86.7	−19.46
EVA/Cell.2.5%	46.05	85.59	−14.37
EVA/Cell.5%	44.7	86.24	−16.59
EVA/Cell.7.5%	45.27	86.26	−15.35
EVA/Cell.10%	46.61	86.37	−16.7

Mechanical properties evaluation

Figure 7 shows the typical stress-strain plots of EVA/cellulose composite systems. Figure 8(a–c) show the effect of cellulose loading on the tensile strength, percentage strain at break, and elastic modulus of EVA/cellulose composites, respectively. From the figures it is clear that the cellulose loaded EVA systems have superior tensile strength compared with neat EVA. Among the composites 7.5 wt % cellulose-loaded EVA shows the highest tensile strength. Elastic modulus has also been found to increase with cellulose content. The increased crystallinity of EVA/cellulose composites observed in XRD plots also support this observation. The percentage strain at break of the composites decreases as the cellulose loading in the composites increases. The physical interaction between the cellulosic filler and EVA matrix can reduce the mobility of the polymeric segments under an applied load.

Transmittance measurement

All the composite films were tested for their transmittance by using a spectrophotometer. It has been observed that there is not much change in the transmittance characteristics of pure EVA and EVA/cellulose composites. The transmittance values of composites and EVA vary between 81 and 84%. Thus the addition of cellulose whiskers makes little difference to the transmittance properties. The composite films have been found to retain their optical clarity reasonably well.

Critical surface tension evaluation

Studies based on contact angle measurements were undertaken for all the composite films. These involved

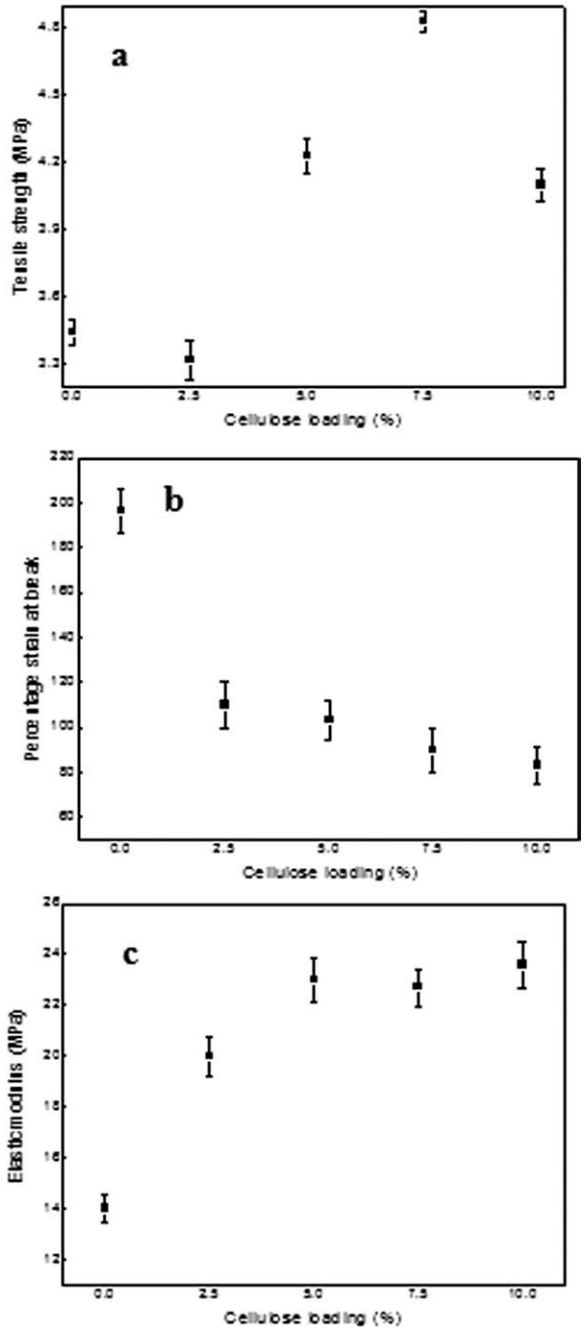

Figure 8 Effect of cellulose loading on the (a) Tensile strength, (b) Percentage strain at break, (c) Elastic modulus of EVA/cellulose composites.

the use of the sessile drop technique, using fluids of known surface tension. From plots of cos θ (θ being the contact angle of each fluid on the polymer sample surface) versus γ_{LV} (surface tension of the liquid–vapor interface), the point of intersection of the line at cos θ = 1 was noted, which is γ_c, the critical wetting tension of the fluid on the surface. The difference in γ_c across all the samples was very small, γ_c values ranging from 25.72 to 26.55 dyn/cm were obtained.

CONCLUSIONS

Composite materials have been prepared by incorporating cellulose whiskers into a poly(ethylene-*co*-vinyl acetate) (EVA) matrix. It was found that the EVA/cellulose composites were more thermally stable than EVA or cellulose alone. In the DSC results, a shift in softening temperature of vinyl acetate in EVA was observed, indicating the development of a favorable interaction between cellulose and vinyl acetate regions of EVA copolymer. The mechanical testing of the samples revealed that 7.5 wt % cellulose loaded EVA offered the highest tensile strength. The elastic modulus was found to increase with the cellulose content whereas percentage strain at break decreased, within the loading range of 0–10 wt %. X-ray diffraction studies showed that EVA/cellulose composites were more crystalline than EVA. The developed composites, since both EVA and cellulose are biocompatible, are being tried to use for biomedical applications.

References

1. Liu, D. Y.; Yuan, X. W.; Battacharya, D.; Easteal, A. J. eXPRESS Polym Lett 2010, 4, 26.
2. Malunka, M. E.; Luyt, A. S.; Krump, H. J Appl Polym Sci 2006, 100, 1607.
3. Dikobe, D. G.; Luyt, A. S. eXPRESS Polym Lett 2009, 3, 19.
4. Favier, V.; Chanzy, H.; Cavaille, J. Y. Macromolecules 1995, 28, 6365.
5. Chazeau, L.; Paillet, M.; Cavaille, J. Y. J Polym Sci B: Polym Phys 1999, 37, 2151.
6. Chazeau, L.; Cavaille, J. Y.; Terech, P. Polymer 1999, 40, 5333.
7. Chazeau, L.; Cavaille, J. Y.; Canova, G.; Dendievel, R.; Boutherin, B. J Appl Polym Sci 1999, 71, 1797.
8. Ljungberg, N.; Bonini, C.; Bortolussi, F.; Boisson, C.; Heux, L.; Cavaille, J. Y. Biomacromolecules 2005, 6, 2732.
9. Samir, M. A. S. A.; Alloin, F.; Gorecki, W.; Sanchez, J. Y.; Dufresne, A. J Phys Chem B 2004, 108, 10845.
10. Samir, M. A. S. A.; Alloin, F.; Sanchez, J. Y.; Dufresne, A. Macromolecules 2004, 37, 4839.
11. Samir, M. A. S. A.; Alloin, F.; Sanchez, J. Y.; Dufresne, A. Polymer 2004, 45, 4149.
12. Angles, M. N.; Dufresne, A. Macromolecules 2000, 33, 8344.
13. Oksman, K.; Mathew, A. P.; Bondeson, D.; Kvien, I. Comp Sci Tech 2006, 66, 2776.
14. Samir, M. A. S. A.; Alloin, F.; Dufresne, A. Biomacromolecules 2005, 6, 612.
15. Heux, L.; Chauve, G.; Bonini, C. Langmuir 2000, 16, 8210.
16. Gousse, C.; Chanzy, H.; Excoffier, G.; Soubeyrand, L.; Fleury, E. Polymer 2002, 43, 2645.
17. Grunert, M.; Winter, W. T. J Polym Environ 2002, 10, 27.
18. Araki, J; Wada, M.; Kuga, S. Langmuir 2001, 17, 21.
19. Samir, M. A. S. A.; Alloin, F.; Sanchez, J. Y.; El Kissi, N; Dufresne, A. Macromolecules 2004, 37, 1386.
20. Viet, D.; Candanedo, S. B.; Gray, D. G. Cellulose 2007, 14, 109.
21. Soudais, Y.; Moga, L.; Blazek, J.; Lemort, F. J Anal Appl Pyrol 2007, 80, 36.
22. Shin, S. C.; Lee, H. J Eur J Pharm Biopharm 2002, 54, 325.
23. Silviya, E. K.; Unnikrishnan, G.; Varghese, S.; Guthrie, J. T. Carbohydr Polym 2010, 80, 852.
24. Alemdar, A.; Sain, M. Comp Sci Tech 2008, 68, 557.